Effective Heating and Improved Confinement Transition in Lower Hybrid Experiment on FT-2 Tokamak

S.I. Lashkul 1), A.B. Altukhov 1), A.D. Gurchenko 1), E.Z. Gusakov 1), V.V. Dyachenko 1), L.A. Esipov 1), M.Yu. Kantor 1), D.V. Kouprienko 1), A.V. Pavlov 2), A.Yu. Popov 1), S.V.Shatalin 2), A.P. Sharpeonok 1), A.Yu. Stepanov 1), E.O.Vekshina 2)

1) A.F.Ioffe Physico-Technical Institute, Politekhnicheskaya 26, 194021, St.Petersburg, Russia
2) St.Petersburg State Polytekhnical University, St.Petersburg, Russia

e-mail: Serguey.Lashkul@mail.ioffe.ru

Abstract. The paper presents the new data on the effective Lower Hybrid Heating (LHH) which has been studied at FT-2 tokamak. The main goal of the experiments is analyze the plasma core parameters, when the Internal Transport Barrier (ITB) during auxiliary LHH and than edge (ETB) Transport Barrier has been observed. The task of this paper is both the presentation of the characteristic features of the edge parameters variation, which was observed at $P_{LHH} = 90 \div 100$kW when the edge transport barrier is formed and the presentation of the first results obtained at enhanced RF power $P(LHH) \approx 2P(OH) = 180$kW. A considerable attention in the recent studies researches was paid to statistical analysis of the edge plasma parameters. The paper presents corresponding data and illustrates dependence change of Probability Distribution Functions (PDFs) of fluctuation induced flux oscillations measured near of the LCFS on HFS and LFS of the plasma core. The new experimental data connected with fluctuation induced flux parameters changes are presented and discussed. In development of the LHH experiment the enhanced additional LH heating $P(LHH) \approx 2P(OH) = 180$kW is applied. Useful increase electron and ion temperatures the same as plasma density are observed. Fast drop down of the H_β spectral line intensity as well as periphery radiation losses decrease indicates at L - H transition. The experiment demonstrates the L – H transition with suppression of the radial fluctuation induced flux near LCFS which observed just with LHH switch on. The new experimental data are presented and discussed.

1. Introduction

The paper presents the new data on the effective Lower Hybrid Heating (LHH) which is used at FT-2 tokamak. As a result of the Lower Hybrid additional Heating and transition into improved confinement the energy confinement time in the post heating phase increases compared to the initial OH phase from τ_{OH}=0.8ms to $\tau_{PostLHH}$= 2.8ms [1, 2]. The task of this paper is both (1) the presentation of the new characteristic features of the edge parameters change, which was studied at $P_{LHH} = P_{OH} = 90 \div 100$kW when the edge transport barrier is formed [1] and (2) the presentation of the first data with enhanced RF power of additional heating corresponding to the twice ohmic power $P_{LHH} \approx 2P_{OH}$=180kW.

(1) The considerable attention in experimental researches of the edge plasma's characteristics is paid to statistical analysis of density and potential fluctuations. In the theory of plasma turbulence it is often assumed that the statistical properties of fluctuating processes are close to the properties of Gaussian random process [3]. Although there are observations of the edge plasma on the many fusion devices, that the time realizations of density and potential have "burst" structures, i.e. they contain the fast density spikes and holes [4, 5]. That is why the probability distribution function (PDF) of the fluctuations may be far from Gaussian PDF at the plasma edge where the large scale fluctuations are not rare events [6]. The PDF of the described intermittent transport [5, 6] is a useful characteristic to describe the dynamics of these large transport events. The statistical analyze of the periphery fluctuation at L –H transition in the FT-2 experiment when $P_{LHH} = P_{OH}$ is considered in the Chapter 2 of the paper.

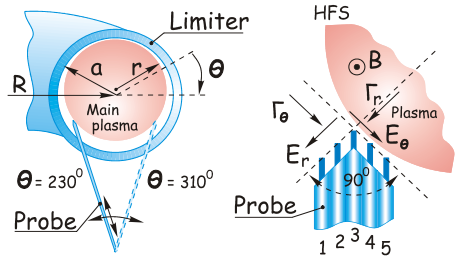

FIG. 1 Multielectrode Langmuir probe arrangement for measurement at Low (LFS, $\theta = 310^0$) and High (HFS, $\theta = 230^0$) Field Sides of characteristic properties of the periphery plasma parameters

(2) In development of the LHH experiment the additional LH heating of the higher power is applied. The main plasma parameter changes measured by unique diagnostics are described and analyzed in the Chapter 3. The discussion of the new characteristics of the observed effective heating and transition into improved confinement mode is given in the end of the Chapter.

2. The statistical properties of the periphery fluctuations at L – H transition on FT-2 tokamak

Statistical properties analysis of plasma density and the particle flux fluctuations are presented for FT-2 tokamak periphery, which was studied at $P_{LHH} = P_{OH} = 90 \div 100$kW. The presented data are obtained by 5 pin Langmuir probe. The experiment is carried out in discharge the following parameters q = 6 (R=0.55m, a_L=0.079m, I_{pl} = 22kA and B_t = 2.2T) [2]. For axial heating the initial central density of the plasma core has to be $n_e(r = 0\ cm) \approx 3{,}5\ 10^{20} m^{-3}$.The RF pulse ($\Delta t_{LH}$ = 5ms, f =920MHz) is applied at the 30th ms of a Δt_{pl} = 50ms plasma shot. During additional LHH the ITB is formed spontaneously a few ms after the RF pulse start. The L-H transition with Edge Transport Barrier (ETB) has been observed after the RF pulse end. Energy confinement time increases during RF pulse from τ_E(OH) = 0.8ms up to τ_E(postLHH) = 2.8 ms when LHH is switched off and L - H transition is observed [1]. As the probe measurements show, L – H transition and ETB formation are associated with negative E_r rise near LCFS after LHH pulse [2, 7]. Experimental scenario and multi pin Langmuir probe arrangement (see Fig. 1) for measurement at Low (LFS, $\theta = 310^0$) and High (HFS, $\theta = 230^0$) Field Sides of characteristic properties of the periphery plasma parameters are described in detail in [2, 7]. The poloidal angle θ shows the probe position in respect to the equatorial outboard midplane in the direction of the electron diamagnetic drift. The plasma core was slightly shifted upward (by 3÷4 mm) to allow probe measurements in the deeper layers of the plasma near LCFS and for some adjustment of the plasma parameters poloidal symmetry. The probes can be moved from limiter shadow and SOL (r ~ 80 – 76mm) up to LCFS region (r~76 – 74 mm) on the shot by shot basis. Observed suppression of the radial fluctuation induced flux $\Gamma_r^{\sim}(t) = C_{n(\sim)E(\sim)}\, c \langle n^{(\sim)2}(t)\rangle^{1/2} \langle E_\theta^{(\sim)2}(t)\rangle^{1/2}/B_\varphi$, during LHH could be caused by decrease of poloidal electric field E_θ, and density $N_e^{\sim}$ oscillations as well as by the reduction of the correlation coefficients $C_{n(\sim)E(\sim)}$.[7] The Fig. 2 illustrates the time behavior of these parameters at plasma periphery for LCFS region ($r = 74mm$) at HFS ($\theta = 230^0$). The correlation coefficient $C_{n(\sim)E(\sim)}$ is depicted for a few probe positions, $r = 74\text{-}77mm$. These data

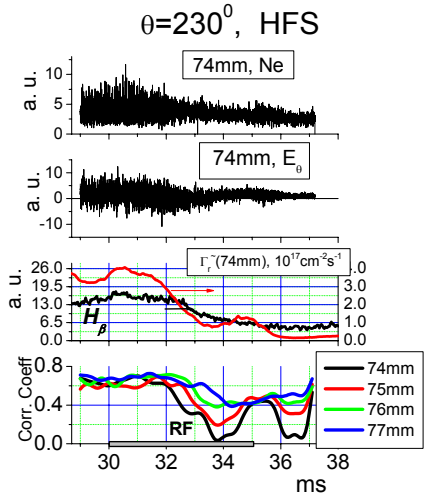

FIG. 2 The time behaviour of the plasma fluctuation periphery parameters at HFS. $\Gamma_r^{\sim}$ is radial fluctuation induced flux averaged over 0.5 ms

show a gradual decreases of the $\Gamma_r^{\sim}(t)$ on the plasma edge when ITB forms at the medium radii (r = *4-5cm, t ~ 32ms*) and therefore after LHH pulse end. Radial fluctuation induced flux $\Gamma_r^{\sim}$ (averaged over 0.5 ms) at the periphery decreases in parallel with H_β radiation. Suppression of radial fluctuation induced transport at plasma column periphery, starting from ITB formation at 32 ms, defines the mechanism of L - H transition, which is observed after LHH pulse end [2, 7].

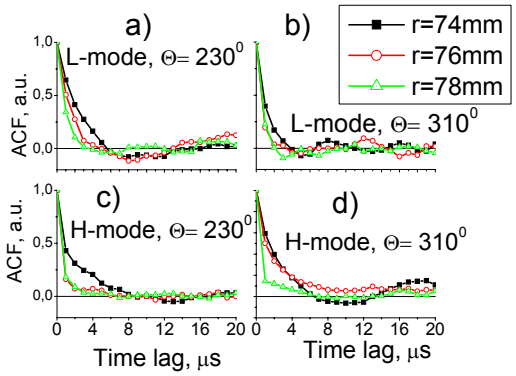

FIG. 3 Change of the Auto Correlation Functions of the saturated ion current oscillations measured at r = 74mm (near of the LCFS), r = 76mm and r = 78mm on HFS and LFS.

Change of the PDF of the observed intermittent transport is a fundamental characteristic to describe the dynamics of these transport processes. At the angle $\theta=230^0$ the three electrodes (1, 2 and 3) of the 5th pin Langmuir probe are located along tangential direction in respect to the plasma cross section [7]. The (4) and (5) pins are located in radial direction. The middle pins (2) and (4) of those electrodes have been used for ion saturation current δI_{sat} measurements. The edge pins (1), (3) and (5) were set at floating potential. In this case, neglecting the electron temperature fluctuations, one can suppose, that : $\delta I_{sat} \propto \delta n$, $\delta\phi_f \propto \delta\phi_{s(space)}$ and density of the radial fluctuation induced flux $\Gamma_r^{\sim}(t)$ is $\delta\Gamma_r \propto \delta I_{sat}(\delta\phi_{1f} - \delta\phi_{3f})$, where $\delta\phi_{1f}$ and $\delta\phi_{3f}$ are floating potentials at the edge pins (1) and (3). The 10^{th} digit analogue-to-digital converter with 1 MHz timing generator is used for probe signal registration. The data are analyzed using the 1 ms (29÷30 ms) time samples of the ion saturation current or fluctuation induced flux for OH (L – mode) and (35÷36) one on the post LH heating period (H-mode). It has been checked if the fluctuations' temporary realizations correspond to the both criterion of a stationary and the criterion of an events' independence.

Analysis of the 1 ms time samples of the ion saturation current and radial fluctuation induced fluxes using the criterion of the inversions shows that stationary hypothesis about could be accepted with 5% significance level [8]. Verification of the "events' independence" was carried out using the Auto Correlation Functions (ACFs). The Fig 3 illustrates the change of the ACFs of the ion saturation current oscillations measured at r = 74mm (near of the LCFS), r = 76mm and r = 78mm on HFS and LFS. One can see, that the Full Width at Half Maximum (FWHM) of the ACFs weakly change during L – H transition and remains ~ 2÷3 ms, which is congruent with 1 mks timing generator numeralization. So, temporary realizations satisfy to the criterion of an events' independence. At the same time the ACF FWHM on the HFS is approximately two times wider than the ACF FWHM on the LFS. There is a decrease of the ACF FWHM's

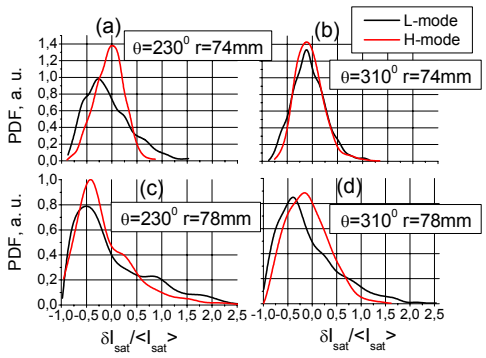

FIG. 4 The PDF of the saturated ion currents for four space points on HFS (a. c) and LFS (b, d).

during displacement outward from the plasma core. The PDF of the ion saturation currents and fluctuation induced fluxes are shown in Fig.4 and Fig. 5 for four spatial points. For the L-mode phase the PDF of the saturated ion currents are characterized by the wide and asymmetric distributions with clear positive non-Gaussian long lag tail, which point out at high event probability of the positive dense plasma spikes. The L – H transition results in the PDF peaking with decrease of the positive non-Gaussian long lag tails. It is typical that the left "tail" of the PDFs (r = 78mm) has the cut-off because the plasma density could be only positive. At the same time at L-H transition there is a symmetrisation of the PDFs near the LCFS (r = 74mm), Fig. 4a and 4b. For both sides (HFS and LFS) the PDFs near LCFS are closer to the Gaussian distribution (Skewness S ~ 0 and Flatness K~3 [5]) than near limiter (r = 78mm) where S > 0 and K-3 > 0

The PDF peaking and symmetrisation as a result of a L – H transition is observed for radial drift fluctuation induced fluxes (Fig. 5). However the shape of the distribution functions on the LFS and the HFS at L – mode is essentially different. On the HFS at L – mode the positive non-Gaussian long lag tails are observed, that indicates a high probability of the extremely large spikes of the outward particle flux. On the LFS the non-Gaussian long lag tails are negative (Fig. 5b and 5d), i.e. the inward particle flux. The presence of the periphery plasma waveform with higher density (filaments, blobs) moving inward to the plasma core has been registered on the LFS of the FT-2 earlier [9].

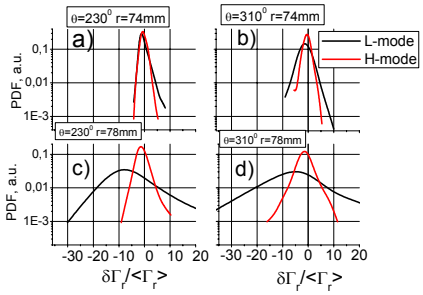

FIG. 5 The PDF of the fluctuation induced fluxes for two space points on HFS and LFS.

So, the analysis of the Langmuir probe measurements permits to determine that statistical properties of the periphery ion saturation current fluctuations and radial drift fluctuation induced fluxes are significantly inhomogeneous both in poloidaly and radial directions. In the L-mode the PDFs of the fluctuations measured at different radial positions and poloidal angles are essentially different from normal (Gaussian) distribution. L – H transition results in significant changes of the statistical characteristics of the periphery fluctuations. The PDFs of the investigated values peak and become more symmetrical. The ion saturation current fluctuations PDF become closer to the normal law (criterion of χ^2 [8]) only in the region directly near to the LCFS (r = 74mm). So, a assumption frequently used in theoretical models that fluctuating parameters correspond to the normal law [3] becomes restricted at the plasma edge. The new experimental investigations and new original procedures developed for the analysis of experimental results are needed. In particular, there is an idea for interpretation of the experimental PDF as a number of the same normal (Gaussian) distributions of turbulent

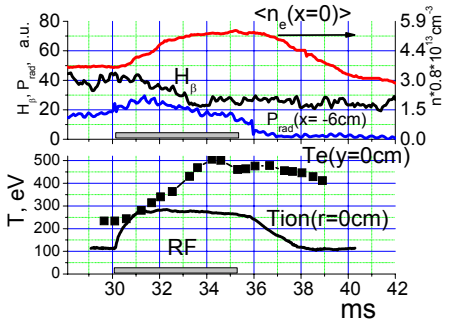

FIG. 6 Here $<n_e(x=0cm)>$ is central line of sight averaged density, $T_e(y=0cm)$ $T_i(r=0cm)$ are central electron and ion temperatures. H_β - spectral line intense. Decrease radiation losses P_{rad} shown for high field side chord X = - 6cm.

fluxes with help of EM – algorithm [6]. Such approach permits to obtain the information about numerous processes, which stimulate the turbulence, and estimate theirs characteristics.

3. Characteristic features of the experiment with enhanced LH additional heating power

In development of the LHH experiment the enhanced additional Lower Hybrid Heating (LHH) is applied. The power of RF pulse P_{LHH} is increased up to $2\,P_{OH} \approx 180$ kW. The experimental scenario is the same as described in the previous Section with the plasma core slightly shifted upward (see Fig. 1). The main plasma parameters are measured by standard and unique diagnostic techniques. Changes of the electron temperature T_e and plasma density n_e are measured by a laser Thomson scattering (TS) diagnostics, respectively and a 2mm interferometer, respectively, $T_{ion}(r)$ is measured by Nuclear Particle Analyzer (NPA). Spectral measurements are made with two monochromators providing observation of the radial impurity distribution in hydrogen plasma as well as measurements of ion temperature and poloidal rotations of plasma by spectral line broadening and Doppler shift of the impurity line radiation [10]. For control of the fast changes of the hydrogen recycling the measurements of profiles of the hydrogen line emission during one short are provided by applying a television video camera (VC) as a radiation detector of the monochromator. SOL parameters are measured by multipin Lengmuir probes. The correlative upper hybrid resonance (UHR) backscattering technique was used for investigation of the small-scale density turbulence at the FT-2 tokamak.

3.1 The main plasma parameter changes

Fig. 6 depicts waveforms of the following main parameter: central (x=0cm) line of sight

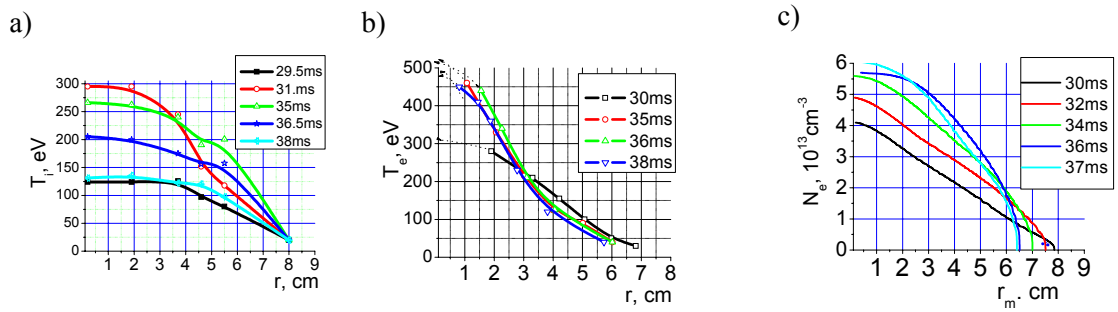

FIG. 7 The profiles of the main parameters against to the magnetic surfaces radii. The data of Langmuir probe for 37 ms is shown by short dot line in Fig. 7c.

averaged density $\langle n_e \rangle$, electron temperature T_e(y=0cm) measured by the (TS) diagnostics at the central position (y=0cm) at the vertical laser probing and central ion temperatures T_i(r=0cm). These parameters rise during RF heating pulse. Fast drop down of the H_β(481.8nm) spectral line intensity as well as the radiation losses decrease shown for a high

TABLE 1 COMPARISON OF THE MAIN PLASMA PARAMETER CHANGES

	$\Delta T_e^{LHH}/T_e^{OH}$	T_i^{LHH}/T_i^{OH}	T_e^{LHH}/T_e^{OH}	$P_{rad}^{LHH}/P_{rad}^{OH}$	N_e^{LHH}/N_e^{OH}
$P^{LHH} = 2P^{OH}$	0.78	2.6	1.8	2.1	1.5
$P^{LHH} = P^{OH}$	0.26	1.9	1.4	1.5	1.24

field side chord x = - 6cm in Fig. 6 indicates L - H transition during RF pulse.
The profiles of these parameters against the magnetic surfaces radii are presented in Fig. 7. It should be noted, that during additional heating a small shift (without any plasma current

disruptions) of the plasma column along the major radius R is observed. The shift of the magnetic surfaces center obtained from interferometer density measurements is taken into account for magnetic surface referencing of the TS electron temperature data presented in Fig. 7b.

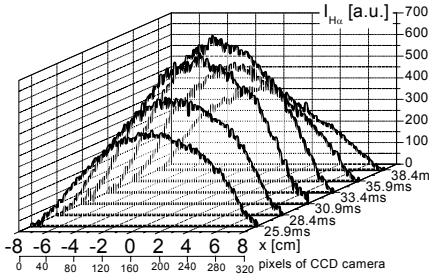

Fig. 8 The H_α (656,3nm) line integral radiation intensity against vertical diameter obtained during one short.

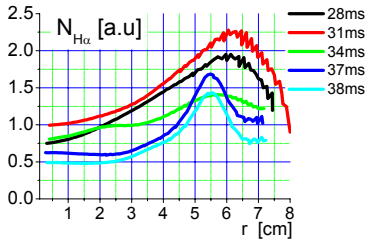

FIG. 9. Calculated per-unit neutral density radial profiles $N_H(r) = (I_{H\alpha}/n_e)kX$ versus to magnetic surface radii

The effect of the higher additional heating, with twice ohmic power $P_{LHH} \approx 2P_{OH}$ is compared with experiments at $P_{LHH} \approx P_{OH}$ [1] (see Table 1). These data indicate fact, that efficiency of the LH heating of the ion component remains approximately the same as at smaller RF power. Furthermore, the central electron temperature increases also and remains for about 5 ms at high level after RF pulse switch off.

The registration of the monochromator outward slit image by the camera has been carried out for control of the fast hydrogen recycling processes. Fig. 8 presents the H_α (656,3nm) line integral radiation intensity against vertical diameter obtained during one shot. As in the case for H_β line there is fast decrease of the spectral line intensity $I_{H\alpha}$ after 34 ms. After inversion of the $I_{H\alpha}(x)$ to $I_{H\alpha}(r)$ the calculated per-unit neutral density radial profiles $N_H(r) = I_{H\alpha}(r)/(n_e(r))kX)$ against the magnetic surface radii demonstrate a fast hydrogen atom density decrease (see Fig. 9) after L – H transition. Here X[cm^3/s] is the excitation rate and k is the geometrical factor. We would like to draw attention to the shift of the maximum of the $N_H(r)$ deeper into the plasma core (see profiles of the 34 – 38 ms), which could be explained by both by spontaneous decrease of hydrogen influx i.e. recycling or by decrease of the minor radius at the L – H transition. The bolometric data also demonstrate fast decrease of the radiation losses from the periphery region of the plasma core (as one can see in the Fig. 7).

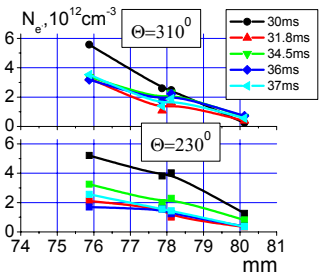

FIG. 10. The SOL plasma density profiles changes

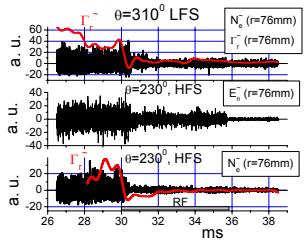

FIG. 11 The poloidal electric field $E_\theta^{\sim}$, density $N_e^{\sim}$ oscillations and the radial fluctuation induced flux $\Gamma_r^{\sim}(t)$ (red lines) near of the LCFS

The decrease of the hydrogen recycling near plasma periphery can be caused by changes of plasma parameters and transport in the SOL. The Fig.10 depict changes of the SOL plasma density at (LFS, $\theta = 310^0$) and (HFS, $\theta = 230^0$) during LHH. Suppression of the poloidal electric field $E_\theta^{\sim}$, density $N_e^{\sim}$ oscillations (frequency band $\Delta f = 0 – 500$kHz) as well as the reduction of the radial fluctuation induced flux $\Gamma_r^{\sim}(t)$ near LCFS are observed non spontaneously (as shown in Fig 2) but just with LHH switch on.

3.2 Plasma core turbulence microwave diagnostics

Suppression of the density turbulence at plasma periphery is also confirmed by microwave diagnostic's measurements. The upper hybrid resonance (UHR) backscattering (BS) technique with of equatorial plane *X*-mode perpendicular probing from high magnetic field side [11] was used for investigating of the small-scale density turbulence at the FT-2 tokamak. This diagnostic is sensitive to fluctuations with radial wave numbers in a wide range $q_r > 2k_{i0}$, where $k_{i0} = 2\pi f_i/c$ is a vacuum wave number of the wave with probing frequency f_i. The UHR BS efficiency has a sharp maximum at $q_r = 2k_{i0}(c/V_{Te})^{1/2}$, which corresponds to BS of the probing wave in its linear conversion point, where V_{Te} is the electron thermal velocity. Typical UHR BS frequency spectrum (*FIG. 11*) was measured in ohmic regime before RF pulse at plasma periphery with the quadrature technique [12]. It consists of intensive low frequency (LF) part $|\Omega/2\pi| < 2$ MHz and asymmetrical spectral wing at -6 dB power level for higher frequencies (HF) $\Omega/2\pi \approx$ (-2..-6) MHz. The LF part has an approximately symmetrical form and relatively small Doppler frequency shift of 0.2-0.5 MHz. The spectral wing's direction in the HF part corresponds to the electron diamagnetic drift direction. The q_r – spectrum of turbulence in ohmic phase was investigated with the correlation technique [13]. The corresponding UHR BS spectrum $I_{q_r,\Omega}$ in logarithmic amplitude scale is shown in *FIG. 12*. The radial wave number corresponding to the spectral maximum is equal to $q_r = 48\pm3$ cm^{-1}, while the wave numbers of the HF spectral wing are much higher and exceeds 75 cm^{-1}.

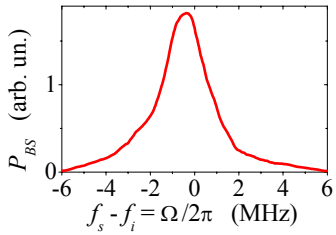

FIG. 11. UHR BS spectrum at r ≈ 6 cm (f_s – scattered frequency).

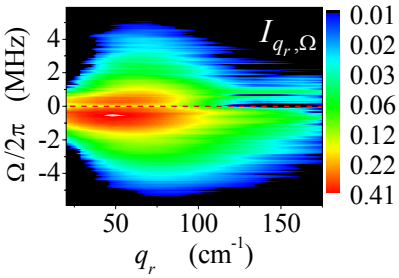

FIG. 12. UHR BS spectrum obtained from correlation measurements.

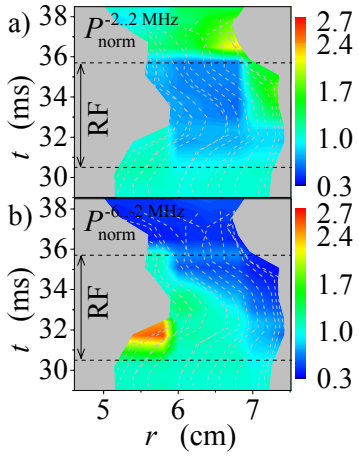

FIG. 13. Evolutions of UHR BS signal profile.

The quadrature technique was applied for investigation of the UHR BS signal's dynamics in ohmic regime with additional RF pulse. Levels of the scattered power integrated in LF (-2..2 MHz) or HF (-6..-2 MHz) ranges were measured for different probing frequencies (54-67 GHz), thus different radial positions from $r = 5$ cm till 7.5 cm. Time evolutions of those profiles normalized to the signal profile at 29 ms (in order to find the influence from LHH only) are shown in *FIG. 13*, where cyan tint corresponds to $P_{norm} = 1$. The UHR positions for fixed f_i are shown on *FIG. 13* by light grey dashed curves, whereas the radial positions inaccessible for the UHR BS are shown by light grey blanks. Evidently the level of the scattered power for LF component of the signal coming from the outer plasma region was nearly halved during the LHH pulse (*FIG. 13a*) that could be explained by the density turbulence level suppression at the plasma periphery. Then after the RF pulse ending, the level of the UHR BS signal increases by a factor of 3-4. The above signal behavior is well correlated with an electron thermal conductivity χ_e dynamics, which was suppressed during the LHH pulse in early experiments [1] and was studied before and after the RF pulse in the present work. As it is seen in *FIG. 14* at $t \approx 36$ ms χ_e is still suppressed everywhere and then starting growth. At $t \approx 37$ ms χ_e reaches the ohmic value for $r > 4.5$ cm and at $t \approx 38$ ms significantly exceeds the ohmic value for $r > 4.3$ cm. At the same time an electron thermal conductivity's level remains less than ohmic value in the hot inner region of the plasma.

It should be stressed that the behavior of the HF turbulence component, corresponding to higher wave numbers, is totally different from the LF signal dynamics (*FIG. 13b*). The area where the HF signal power is suppressed expands starting from the moment $t = 31$ ms from the very edge of the plasma to the inner regions. From $t = 36.5$ ms the HF signal become suppressed in the whole region which is accessible for the UHR BS measurements. Such puzzling signal's behavior could be explained supposing that these high frequency and extremely small-scale fluctuations belong to the ETG-mode turbulence as it is seen in Fig. 15. The ETG-mode threshold condition [14] $L_T < 1.25\, L_n$, where L_T (*FIG. 15a*) and L_n (*FIG. 15b*) are electron temperature and density scale lengths, was overcome only in the small area for $r < 6.5$ cm from $t = 30$ ms till $t = 34$ ms, exactly where the HF signal power growth was observable (*FIG. 13b*). Violation of the threshold criterion in remaining areas is well correlated with suppression of the HF signal.

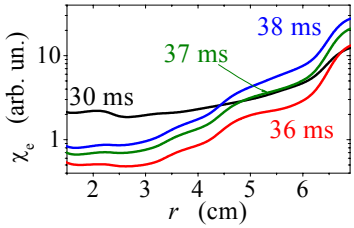

FIG. 14. Electron thermal conductivity profiles.

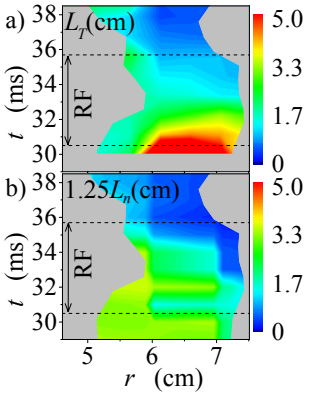

FIG. 15. L_T and L_n evolutions.

Summarizing results of the UHR BS measurements we would like to state that two components were observable in the signal that could be attributed to two different small-scale modes of drift turbulence. The first one, corresponding to density turbulence with frequency $-2\ \text{MHz} < \Omega < 2\ \text{MHz}$ and radial wave length $\Lambda_r \approx 0.13$ cm is dominating in the signal and well correlated with an electron thermal conductivity level on plasma periphery. The amplitude of the second component, corresponding to fluctuations with $\Lambda_r < 0.08$ cm and $-6\ \text{MHz} < \Omega < -2\ \text{MHz}$, experiences the significant growth when the ETG mode instability condition $L_T < 1.25\, L_n$ is fulfilled, and is strongly suppressed in the opposite case.

In conclusion we would like to underline, that the efficiency of the LH heating of the ion component at doubling RF power ($P_{LHH} \approx 2P_{OH} = 180$kW) remains the same high. The electron temperature rise is explained by the thermal conductivity decreases (see Fig. 14). The L – H transition with hydrogen recicling decrease and density turbulence suppression are observed and will be subject for next study.

This work supported by NWO-RFBR 047.016.015, RFFR 04-02-16534, 05-02-17761, 05-02-16569 and RF Schools grant 5149.2006.2

References

1. S.I. Lashkul, et al. Plasma Physics Reports. 2001 Vol. 27 No. 12. pp.1001-1010
2. S.I. Lashkul, A.B.Altukhov et al. Czechoslovak J. of Physics (2005) 55 (3) 341 – 348
3. Krommers J. Physics Reports 369 (2002) p. 1
4. D.L. Rudakov, et al. Plasma Phys. Control. Fusion 44 (2002) 717
5. Kirnev G.S. et al. // Nucl. Fusion. V.**45**. 2005. P.459
6. N.N. Skvortsova, et. al. Plasma Phys. Control. Fusion 48 (2006) A393
7. S.I. Lashkul, et al. 32th EPS Conf. on Contr. Fus. and Pl.Phys. Tarragona, (2005) P-4.046
8. Bendat J., Persol A. Application Study of Random Data. M.: Mir. 1989, P.P.540.
9. S.I. Lashkul et al. Pl. Phys. Reports, V. 32, N5 2006 p. 353
10. S.I. Lashkul, et. al. Plasma Phys. Control. Fusion 44 (2002) 653
11. Altukhov, A.B., et al., Proc. 31 EPS Conf. on Contr. Fus. and Pl.Phys. London (2004), ECA 28B, P-1.173.
12. Altukhov, A.B., et al., Proc. 30 EPS Conf. on Contr. Fus. and Pl.Phys. St.-Petersburg (2003), ECA 27A, P-4.170pd.
13. Gusakov, E.Z., et al., Plasma Phys. Control. Fusion **48** (2006) A371.
14. Jenko, F., Dorland, W., Hammett, G.W., Phys. Plasmas **8** (2001) 4096.